Centrum voor Wiskunde en Informatica

REPORT *RAPPORT*

Preconditioning and multigrid for Euler flows with low-subsonic regions

B. Koren

Department of Numerical Mathematics

Report NM-R9412 June 1994

CWI is the National Research Institute for Mathematics and Computer Science. CWI is part of the Stichting Mathematisch Centrum (SMC), the Dutch foundation for promotion of mathematics and computer science and their applications.
SMC is sponsored by the Netherlands Organization for Scientific Research (NWO). CWI is a member of ERCIM, the European Research Consortium for Informatics and Mathematics.

Copyright © Stichting Mathematisch Centrum
P.O. Box 94079, 1090 GB Amsterdam (NL)
Kruislaan 413, 1098 SJ Amsterdam (NL)
Telephone +31 20 592 9333
Telefax +31 20 592 4199

Preconditioning and Multigrid for Euler Flows with Low-Subsonic Regions

Barry Koren
CWI
P.O. Box 94079, 1090 GB Amsterdam, The Netherlands

Abstract

For subsonic flows and upwind-discretized, linearized 1-D Euler equations, the smoothing behavior of multigrid-accelerated point Gauss-Seidel relaxation is investigated. Error decay by convection over domain boundaries is also discussed. A fix to poor convergence rates at low Mach numbers is sought in replacing the point relaxation applied to unconditioned Euler equations, by locally implicit "time" stepping applied to preconditioned Euler equations. The locally implicit iteration step is optimized for good damping of high-frequency errors. Numerical inaccuracy at low Mach numbers is also addressed. Arguments are given why in the present case it is not a necessity to solve this accuracy problem.

AMS Subject Classification (1991): 65N12, 65N15, 65N22, 65N55, 76G25, 76M25.
Keywords and Phrases: subsonic flows, Euler equations, multigrid methods, preconditioning matrices, convergence and accuracy.
Note: The research reported was performed in the framework of the BRITE-EURAM Aeronautics R&D Programme of the European Communities (Contract No. AER2-CT92-0040).

1 Introduction

Mathematical theory of subsonic gas flows is relatively undeveloped in comparison with that of transonic, supersonic and hypersonic flows. An indication of this is the small amount of literature that is available on subsonic gas dynamics. Whereas various text books exist, exclusively dealing with the mathematics of either transonic, supersonic or hypersonic gas flows, for the subsonic case we only know a few book chapters (e.g. Chapters 2 and 3 from [1], and Chapter 2 from [6]). At present, research in the subsonic flow regime is at a rapid pace, particularly as far as it concerns numerical computations in the incompressible limit. The present paper contributes to this development. In it, the flows of interest are not flows with uniformly low Mach numbers (i.e. flows with $M \ll 1$ throughout almost the entire computational domain), but flows with *locally* low Mach numbers (flows with small stagnation regions and - particularly - for Navier-Stokes extensions: flows with thin boundary layers and wakes).

Since about a decade, various multigrid methods exist that give good convergence rates for steady Euler-flow computations at high-subsonic inflow Mach numbers (see Chapter 9 from [14] for an overview). For decreasing inflow Mach numbers, or enlarging low-subsonic flow regions, convergence rates are known to become less good. This decrease is not specific for multigrid methods, but seems to hold for any solution method. The cause has to be sought in the continuous Euler equations, in their increasing stiffness (i.e. in their increasing disparity of wave speeds) at decreasing subsonic Mach numbers. With the application of single-grid, explicit time stepping schemes in mind, various fixes have been proposed already for this stiffness problem. See [11] for a review of this. An early research paper is [5]. In it, for the Jacobian of the 1-D Euler equations, the preconditioning matrix is given which completely equalizes the three wave speeds $u-c$, u and $u+c$. Further, the paper gives preconditioning matrices for the 2-D and 3-D Euler equations. Besides convergence problems, for decreasing Mach numbers also accuracy problems arise [12, 13]. Whereas the convergence problems are intrinsicly related to the *continuous* Euler equations (to their stiffness), the accuracy problems hold for the *discretized* equations (independent of whether the discretization is central or upwind).

Report NM-R9412
ISSN 0169-0388
CWI
P.O. Box 94079, 1090 GB Amsterdam, The Netherlands

In the present paper, we will mainly focus on the stiffness problem. It is expected that solution methods other than explicit time stepping schemes may also profit from preconditioning matrices such as those proposed in [5]. Led by this expectation, we will optimize a multigrid accelerated, locally implicit iteration method, applied to subsonic, preconditioned Euler equations. To start with, in Section 2, the continuous, unconditioned equations and their discretization are introduced. In Section 3, first a smoothing analysis is given of point Gauss-Seidel relaxation for the discrete equations, and next a discussion is made of error convection across domain boundaries. It is shown that for low Mach numbers, the convergence properties are poor. In Section 4, it is made clear that for flows with uniformly low Mach numbers, numerical accuracy may be poor as well. Since the latter flows are not our interest, in Section 5 a 1-D preconditioning matrix is derived which is only meant for removing stiffness and not for also improving low-Mach-number inaccuracy. In Section 6, a simple way of implementing the preconditioning matrix is discussed. At the end of Section 6 we arrive at the discrete, preconditioned system to be solved. The system contains a free parameter: a locally implicit iteration step, which is optimized for smoothing. The optimization is done in Section 7, through local-mode analysis applied to the upwind-discretized, linearized, preconditioned 1-D Euler equations. In Section 8, the error smoothing and error convection of the locally implicit iteration are verified.

2 The equations

2.1 Continuous equations

Consider the 1-D Euler equations

$$\frac{\partial Q}{\partial t} + \frac{\partial f(Q)}{\partial x} = 0, \tag{1a}$$

with Q the conservative state vector

$$Q = \begin{pmatrix} \rho \\ \rho u \\ \rho e \end{pmatrix}, \tag{1b}$$

$f(Q)$ the corresponding flux vector

$$f(Q) = \begin{pmatrix} \rho u \\ \rho u^2 + p \\ \rho u(e + \frac{p}{\rho}) \end{pmatrix}, \tag{1c}$$

and e the internal energy, which for a perfect gas reads

$$e = \frac{1}{\gamma - 1}\frac{p}{\rho} + \frac{1}{2}u^2. \tag{1d}$$

Linearization of (1a) with respect to the conservative variables yields

$$\frac{\partial Q}{\partial t} + \frac{\mathrm{d}f}{\mathrm{d}Q}\frac{\partial Q}{\partial x} = 0, \tag{2a}$$

$$\frac{\mathrm{d}f}{\mathrm{d}Q} = \begin{pmatrix} 0 & 1 & 0 \\ \frac{\gamma-3}{2}u^2 & (3-\gamma)u & \gamma - 1 \\ \frac{\gamma-2}{2}u^3 - \frac{1}{\gamma-1}uc^2 & \frac{(3-2\gamma)}{2}u^2 + \frac{1}{\gamma-1}c^2 & \gamma u \end{pmatrix}, \tag{2b}$$

where $c^2 = \sqrt{\gamma p/\rho}$. To simplify the analysis, following Turkel [10], the transformation from conservative variables Q to non-conservative (entropy) variables q is made:

$$\mathrm{d}q \equiv \begin{pmatrix} \frac{1}{\rho c}\mathrm{d}p \\ \mathrm{d}u \\ \mathrm{d}p - c^2 \mathrm{d}\rho \end{pmatrix}. \tag{3}$$

The corresponding transformation matrix

$$\frac{\mathrm{d}Q}{\mathrm{d}q} = \begin{pmatrix} \frac{\rho}{c} & 0 & -\frac{1}{c^2} \\ \frac{\rho u}{c} & \rho & -\frac{u}{c^2} \\ \frac{1}{2}\frac{\rho u^2}{c} + \frac{1}{\gamma-1}\rho c & \rho u & -\frac{1}{2}\frac{u^2}{c^2} \end{pmatrix} \tag{4}$$

brings equation (1a) into the analytically much more tractable form

$$\frac{\partial q}{\partial t} + A\frac{\partial q}{\partial x} = 0, \tag{5a}$$

$$A = \frac{\mathrm{d}q}{\mathrm{d}Q}\frac{\mathrm{d}f}{\mathrm{d}Q}\frac{\mathrm{d}Q}{\mathrm{d}q} = \begin{pmatrix} u & c & 0 \\ c & u & 0 \\ 0 & 0 & u \end{pmatrix}. \tag{5b}$$

2.2 Discrete equations

We make a first-order upwind, cell-centered finite-volume discretization of the space operator in (5a). Then, the semi-discrete equation in cell Ω_i (with mesh size h) reads

$$h\frac{\partial q_i}{\partial t} + A^+(q_i - q_{i-1}) + A^-(q_{i+1} - q_i) = 0, \tag{6}$$

with i running in positive x-direction, and with A^+ and A^- the matrices corresponding with the positive and negative eigenvalues of matrix A:

$$A^+ = R_A \Lambda_A^+ R_A^{-1}, \tag{7a}$$

$$A^- = R_A \Lambda_A^- R_A^{-1}. \tag{7b}$$

With $\Lambda_A = \mathrm{diag}(u-c, u, u+c)$, it holds

$$R_A = \begin{pmatrix} 1 & 0 & 1 \\ -1 & 0 & 1 \\ 0 & 1 & 0 \end{pmatrix}, \tag{8}$$

and, hence, for subsonic flow in positive x-direction, $0 < u < c$:

$$A^+ = \frac{1}{2}\begin{pmatrix} u+c & u+c & 0 \\ u+c & u+c & 0 \\ 0 & 0 & 2u \end{pmatrix}, \tag{9a}$$

$$A^- = \frac{1}{2}\begin{pmatrix} u-c & c-u & 0 \\ c-u & u-c & 0 \\ 0 & 0 & 0 \end{pmatrix}. \tag{9b}$$

3 Convergence

3.1 Convergence through error smoothing

Applying point Gauss-Seidel relaxation to find the steady solution of (6), for successively a downstream and upstream relaxation sweep the iteration formulae are

$$|A|(q_i^{n+1} - q_i^n) = -A^+(q_i^n - q_{i-1}^{n+1}) - A^-(q_{i+1}^n - q_i^n), \tag{10a}$$

$$|A|(q_i^{n+2} - q_i^{n+1}) = -A^+(q_i^{n+1} - q_{i-1}^{n+1}) - A^-(q_{i+1}^{n+2} - q_i^{n+1}), \tag{10b}$$

with $|A| \equiv A^+ - A^-$ and n the relaxation sweep counter. To investigate the smoothing properties we introduce the local solution error

$$\delta_i^n = q_i^* - q_i^n, \tag{11a}$$

and the Fourier form

$$\delta_i^n = D^n \mathrm{e}^{\mathrm{i}\theta i}, \quad |\theta| \in \left[\frac{\pi}{2}, \pi\right], \tag{11b}$$

with q_i^* the exact local solution, D^n the amplitude vector (D_1^n, D_2^n, D_3^n) and $\mathrm{e}^{\mathrm{i}\theta i}$ the (scalar) mode. Keeping the coefficient matrices in (10a) and (10b) frozen, with (11a) and (11b), it follows for the amplification matrices $\mathcal{M}_{\mathbf{downstream}}$ and $\mathcal{M}_{\mathbf{upstream}}$:

$$\mathcal{M}_{\mathbf{downstream}} = -\left(-\mathrm{e}^{-\mathrm{i}\theta}A^+ + |A|\right)^{-1} \mathrm{e}^{\mathrm{i}\theta}A^-, \tag{12a}$$

$$\mathcal{M}_{\mathbf{upstream}} = \left(\mathrm{e}^{\mathrm{i}\theta}A^- + |A|\right)^{-1} \mathrm{e}^{-\mathrm{i}\theta}A^+. \tag{12b}$$

Substituting A^+ and A^- we find the solution-independent matrices

$$\mathcal{M}_{\mathbf{downstream}} = \frac{1}{2}\begin{pmatrix} \mathrm{e}^{\mathrm{i}\theta} & -\mathrm{e}^{\mathrm{i}\theta} & 0 \\ -\mathrm{e}^{\mathrm{i}\theta} & \mathrm{e}^{\mathrm{i}\theta} & 0 \\ 0 & 0 & 0 \end{pmatrix}, \tag{13a}$$

$$\mathcal{M}_{\mathbf{upstream}} = \frac{1}{2}\begin{pmatrix} \mathrm{e}^{-\mathrm{i}\theta} & \mathrm{e}^{-\mathrm{i}\theta} & 0 \\ \mathrm{e}^{-\mathrm{i}\theta} & \mathrm{e}^{-\mathrm{i}\theta} & 0 \\ 0 & 0 & 2\mathrm{e}^{-\mathrm{i}\theta} \end{pmatrix}, \tag{13b}$$

with spectral radii

$$\rho(\mathcal{M}_{\mathbf{downstream}}) = |\mathrm{e}^{\mathrm{i}\theta}| = 1, \quad \forall|\theta| \in \left[\frac{\pi}{2}, \pi\right], \tag{14a}$$

$$\rho(\mathcal{M}_{\mathbf{upstream}}) = |\mathrm{e}^{-\mathrm{i}\theta}| = 1, \quad \forall|\theta| \in \left[\frac{\pi}{2}, \pi\right]. \tag{14b}$$

(Since the matrices (13a) and (13b) are symmetric, the spectral norms, which determine the smoothing properties for $n = 1$, are identical to the spectral radii.) Note that in case of a symmetric sweep, according to this Fourier analysis, one has perfect smoothing: $\mathcal{M}_{\mathbf{upstream}}\mathcal{M}_{\mathbf{downstream}} = 0$. However, in case of subsonic flow with non-periodic boundary conditions, one generally has error reflections at the outflow boundary when still iterating. Therefore this theoretical, perfect smoothing result is not realistic and therefore we prefer to consider the downstream and upstream amplification matrices separately. However, for the two separate sweeps, the smoothing factors (14a) and (14b) are surprising as well. They are in contradiction with numerical findings; for e.g. standard, high-subsonic airfoil-flow computations, one generally observes good multigrid convergence. A first explanation of this contradictory result is that care has to be taken in interpreting (14a) and (14b); the frozen coefficients assumption generally loses its validity for high-subsonic Mach numbers. As opposed to this, for low-subsonic Mach numbers it seems a reasonable assumption (e.g., for $\lim_{M\downarrow 0}$, ρ becomes constant).

3.2 Convergence through error convection

A second explanation of the contradictory convergence estimate for high-subsonic flows in the general case of non-periodic boundary conditions is that for the downstream and upstream sweep separately, local-mode analysis solely is just too pessimistic. For non-periodic high-subsonic flow computations, additional error decay through advection over the domain boundaries may be of significant importance and may therefore not be neglected. Note herewith that point Gauss-Seidel relaxation can be interpreted as locally implicit time stepping at an infinitely large time step, which with non-zero wave propagation speeds $u - c$, u and $u + c$, implies a significant beneficial influence on convergence. This phenomenon of solution errors being expelled out of the computational domain by convection may next explain the poor multigrid performance for low-subsonic flows. In spite of the infinitely large time step associated with point Gauss-Seidel relaxation, for $\lim_{M\downarrow 0}$, the propagation of entropy errors and therefore their expulsion, may well start to stagnate.

4 Accuracy

4.1 Well-posedness continuous equations

For $\lim_{M\downarrow 0}$, exact solutions of the continuous Euler equations are assumed to converge to the corresponding, exact, incompressible flow solutions. (Compressible flow in the incompressible limit is assumed to be a regular perturbation of incompressible flow.) As a support for this, see e.g. the perturbation theory analysis of slightly compressible flow past a circle in Chapter 2 of [2]. The singularity occurring for $\lim_{M\downarrow 0}$ is not known to cause general non-uniqueness problems; as opposed to for $\lim_{M\rightarrow 1}$ [7], for $\lim_{M\downarrow 0}$ boundary-value problems are not known to become ill-posed.

4.2 Inaccuracy discrete equations

Accuracy problems for $\lim_{M\downarrow 0}$ do arise in the discrete case. The inaccuracy can be analyzed through the modified equation corresponding with (5a)-(5b), discretized through e.g. a first-order accurate flux-difference splitting scheme (such as Osher's [8] or Roe's [9]). The corresponding modified equation reads

$$\frac{\partial q}{\partial t} + A\frac{\partial q}{\partial x} = h\frac{\partial}{\partial x}\left(|A|\frac{\partial q}{\partial x}\right). \tag{15}$$

With

$$|A| = \begin{pmatrix} c & u & 0 \\ u & c & 0 \\ 0 & 0 & u \end{pmatrix}, \tag{16}$$

the numerical diffusion term in the right-hand side of (15) can be written out as

$$h\frac{\partial}{\partial x}\left(|A|\frac{\partial q}{\partial x}\right) = h\left[\left\{\frac{\partial u}{\partial x}\begin{pmatrix} \frac{1}{M} & 1 & 0 \\ 1 & \frac{1}{M} & 0 \\ 0 & 0 & 1 \end{pmatrix} + u\frac{\partial}{\partial x}\begin{pmatrix} \frac{1}{M} & 1 & 0 \\ 1 & \frac{1}{M} & 0 \\ 0 & 0 & 1 \end{pmatrix}\right\}\frac{\partial q}{\partial x} + |A|\frac{\partial^2 q}{\partial x^2}\right]. \tag{17}$$

It appears that for $\lim_{M\downarrow 0}$ and with h fixed and $\frac{\partial u}{\partial x}$ and $\frac{\partial p}{\partial x}$ non-zero, the numerical diffusion term in system (15) becomes infinitely large for the first two equations.

5 Preconditioning

5.1 Removing stiffness

For a detailed account of this topic we refer to [5]. For the condition K of A over the entire subsonic flow regime, it holds

$$K(A) = \max\left(\frac{1+M}{M}, \frac{1+M}{1-M}\right), \quad M \equiv \frac{|u|}{c} \in (0,1), \tag{18}$$

see also Figure 1. At $M = 0$ and $M = 1$, A is singular. Preconditioning A (by premultiplying it) with the 3×3-matrix P transforms equation (5a) into

$$\frac{\partial q}{\partial t} + PA\frac{\partial q}{\partial x} = 0. \tag{19}$$

For general P, the possibility of doing time-accurate calculations is lost. When solving steady problems, this is of no concern. P should at least remove the static and sonic singularity. In the ideal case, P leads to the situation: (i) that $K(PA) = 1$ over the entire subsonic Mach-number range, and (ii) that PA yields two downstream waves and one upstream wave. Satisfaction of the second property, conservation of the propagation directions of the three waves, avoids a change of numbers of boundary conditions to be imposed at in- and outlet. This property is satisfied by taking P positive definite, which implies that P must be symmetric.

A common choice for P is

$$P = \frac{1}{w}|A|^{-1}, \tag{20}$$

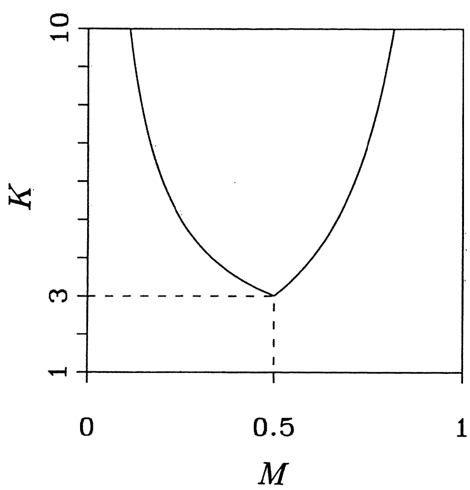

Figure 1: Condition of derivative matrix A as a function of the Mach number.

with w some propagation speed that can still be chosen. With (20) one has $\Lambda_{PA} = \text{diag}(-w, w, w)$. In multi-D, perfect subsonic preconditioning is not possible. For 2-D subsonic Euler flows and for $dq = (\frac{1}{\rho c}dp, du, dv, dp - c^2 d\rho)^T$, the following preconditioning matrix is proposed in [5]:

$$P = \begin{pmatrix} \frac{M^2}{\sqrt{1-M^2}} & \frac{-M}{\sqrt{1-M^2}} & 0 & 0 \\ \frac{-M}{\sqrt{1-M^2}} & \frac{1}{\sqrt{1-M^2}} + 1 & 0 & 0 \\ 0 & 0 & \sqrt{1-M^2} & 0 \\ 0 & 0 & 0 & 1 \end{pmatrix}. \tag{21}$$

The 3-D subsonic preconditioning matrix proposed in [5] is very much the same as (21). Our practical interest lies in doing 2-D and 3-D computations. However, since already in 2-D, local-mode analysis for the full Euler equations is hard and does not lead to transparent results, we do the analysis for the 1-D Euler equations, with as preconditioning matrix a 1-D version of 2-D P (21). We proceed by deriving such a 1-D P.

No symmetric P exists which yields a perfectly conditioned, diagonal matrix, such as $\text{diag}(-w, w, w)$ with w the equalized wave speed. Striving for the almost diagonal form

$$PA = \begin{pmatrix} -w & 0 & 0 \\ \hat{w} & w & 0 \\ 0 & 0 & w \end{pmatrix}, \tag{22}$$

which still satisfies $K(PA) = 1$, $\forall M \in (0,1)$, a symmetric 1-D version of (21) can be found. For $w = u$, it follows

$$P = \begin{pmatrix} \frac{M^2}{1-M^2} & \frac{-M}{1-M^2} & 0 \\ \frac{-M}{1-M^2} & \frac{1}{1-M^2} + 1 & 0 \\ 0 & 0 & 1 \end{pmatrix} \tag{23}$$

(and, unimportant, $\hat{w} = 2c$). Since entropy propagates with the flow speed, just as in (21), the entropy equation is left unchanged. Note that P according to (23) is positive-definite; for $M \in (0,1)$ its three eigenvalues are all positive: $\lambda_1 = 1$ and $\lambda_{2,3} = \frac{1 \pm \sqrt{1-M^2+M^4}}{1-M^2} > 0$, $\forall M \in (0,1)$. Also still note the freedom in the derivation of this preconditioning matrix. E.g., another w could have been chosen; $w = u + c$ would have yielded

$$P = \begin{pmatrix} \frac{M}{1-M} & \frac{-1}{1-M} & 0 \\ \frac{-1}{1-M} & \frac{2-M^2}{M(1-M)} & 0 \\ 0 & 0 & \frac{1+M}{M} \end{pmatrix}. \tag{24}$$

Moreover, instead of preconditioning, postconditioning could have been applied. The difference between pre- and postconditioning can be clarified by considering the auxiliary equation $A\frac{dq}{dx} = r$. Preconditioning this equation ($PA\frac{dq}{dx} = r$) is identical to right-hand side transformation ($A\frac{dq}{dx} = P^{-1}r$), whereas postconditioning ($AP\frac{dq}{dx} = r$) can be interpreted as solution transformation. Postconditioning (5a) by a symmetric P such that

$$AP = \begin{pmatrix} -u & 0 & 0 \\ \hat{w} & u & 0 \\ 0 & 0 & u \end{pmatrix}, \tag{25}$$

leads to

$$P = \begin{pmatrix} -\frac{M^2-2}{M^2-1} & -\frac{M}{M^2-1} & 0 \\ -\frac{M}{M^2-1} & \frac{M^2}{M^2-1} & 0 \\ 0 & 0 & 1 \end{pmatrix}. \tag{26}$$

Interpreting this postconditioning matrix as a solution transformation matrix $\frac{d\tilde{q}}{dq}$, we get

$$d\tilde{q} = \begin{pmatrix} -\frac{M^2-2}{M^2-1}\frac{1}{\rho c}dp - \frac{M}{M^2-1}du \\ -\frac{M}{M^2-1}\frac{1}{\rho c}dp + \frac{M^2}{M^2-1}du \\ dp - c^2 d\rho \end{pmatrix}. \tag{27}$$

Physical interpretation of the first two components of $d\tilde{q}$ is not trivial. In the remainder we consider preconditioning according to (23).

5.2 Concerning inaccuracy

A partial fix to the discrete accuracy problem discussed in Section 4.2, is to make the discretization second-order accurate. (In practical computations, the discretization will be at least second-order accurate anyway.) Of course, as long as the two limits $M \downarrow 0$ and $h \downarrow 0$ are independent (and as long as the discretization method is not exact), formally the accuracy problem remains to exist. A subsequent partial fix would then be to take the mesh size appropriately dependent on the Mach number.

A real fix is to exploit the freedom still existing in the choice of the preconditioning matrices for removing the stiffness problem. By first preconditioning:

$$\frac{\partial q}{\partial t} + PA\frac{\partial q}{\partial x} = 0, \tag{28}$$

and next discretizing (with e.g. a first-order accurate flux-difference splitting scheme), one gets the modified equation

$$\frac{\partial q}{\partial t} + PA\frac{\partial q}{\partial x} = \frac{\partial}{\partial x}\left(|PA|\frac{\partial q}{\partial x}\right), \tag{29}$$

which is identical to

$$P^{-1}\frac{\partial q}{\partial t} + A\frac{\partial q}{\partial x} = P^{-1}\frac{\partial}{\partial x}\left(|PA|\frac{\partial q}{\partial x}\right). \tag{30}$$

For flow computations at uniformly low Mach numbers, the challenge is to get rid of both the stiffness and the accuracy problem by a single preconditioning matrix P. Such double-edged preconditioning matrices are expected to become available soon [12]. Discretization of (28) requires the incorporation of a space discretization scheme which is modified for the preconditioning (both at the interior and the boundary cell faces). Further, in multigrid contexts the residual transfer has to be reconsidered, in order to maintain the Galerkin property and hence good multigrid convergence [4]. Since uniformly low-Mach-number flows are not our present interest, we will not apply the preconditioning in the form (28). (For computations in which the Mach number is not uniformly low, the accuracy problems occurring for $\lim_{M\downarrow 0}$ are local, and hence no reduction of global solution accuracy is expected to be found.)

6 Implementing the preconditioning

By implementing the preconditioning as

$$P^{-1}\frac{\partial q}{\partial t} + A\frac{\partial q}{\partial x} = 0, \tag{31a}$$

with P^{-1} the inverse of (23):

$$P^{-1} = \begin{pmatrix} \frac{2-M^2}{M^2} & \frac{1}{M} & 0 \\ \frac{1}{M} & 1 & 0 \\ 0 & 0 & 1 \end{pmatrix}, \tag{31b}$$

the original space discretization scheme can still be applied (simply because the space operator is still original). Steady-state solutions will therefore be identical to those belonging to the unconditioned equations (5a) and (15). The conservative form corresponding with (31a) reads

$$\frac{\mathrm{d}Q}{\mathrm{d}q}P^{-1}\frac{\partial q}{\partial t} + \frac{\partial f(Q)}{\partial x} = 0. \tag{32}$$

Discretizing (32) by a first-order upwind finite-volume method, and denoting the numerical flux function which approximates cell-face flux $f(q_{i+\frac{1}{2}})$ by $F(q_i, q_{i+1})$, for cell Ω_i the semi-discrete equation reads

$$\int_{\Omega_i} \frac{\mathrm{d}Q}{\mathrm{d}q}P^{-1}\frac{\partial q}{\partial t}\mathrm{d}x + (F(q_i, q_{i+1}) - F(q_{i-1}, q_i)) = 0. \tag{33}$$

Given the good smoothing properties of point Gauss-Seidel relaxation in the multigrid computation of high-subsonic, transonic and supersonic flows, in choosing the time discretization for (33) we deviate as little as possible from this trusty smoother, by applying: locally implicit time stepping in a Gauss-Seidel fashion. Hence, as fully discrete equation in cell Ω_i, for a downstream and upstream sweep respectively, it follows:

$$\left[\frac{h}{\Delta t}\frac{\mathrm{d}Q}{\mathrm{d}q}(q_i^n)P^{-1}(M_i^n) + \frac{\partial F(q_i^n, q_{i+1}^n)}{\partial q_i^n} - \frac{\partial F(q_{i-1}^{n+1}, q_i^n)}{\partial q_i^n}\right](q_i^{n+1} - q_i^n) = F(q_{i-1}^{n+1}, q_i^n) - F(q_i^n, q_{i+1}^n), \tag{34a}$$

$$\left[\frac{h}{\Delta t}\frac{\mathrm{d}Q}{\mathrm{d}q}(q_i^{n+1})P^{-1}(M_i^{n+1}) + \frac{\partial F(q_i^{n+1}, q_{i+1}^{n+2})}{\partial q_i^{n+1}} - \frac{\partial F(q_{i-1}^{n+1}, q_i^{n+1})}{\partial q_i^{n+1}}\right](q_i^{n+2} - q_i^{n+1}) = F(q_{i-1}^{n+1}, q_i^{n+1}) - F(q_i^{n+1}, q_{i+1}^{n+2}). \tag{34b}$$

The time step Δt (which due to the preconditioning is not identical to physical time stepping) is still amenable to optimization. In the next section it will be optimized for smoothing.

7 Optimization locally implicit iteration step

For simplicity, smoothing optimization of Δt from (34a) and (34b) is done for the non-conservative, frozen-coefficient variants of both equations, i.e. for:

$$\left(\frac{h}{\Delta t}P^{-1} + |A|\right)(q_i^{n+1} - q_i^n) = -A^+(q_i^n - q_{i-1}^{n+1}) - A^-(q_{i+1}^n - q_i^n), \tag{35a}$$

$$\left(\frac{h}{\Delta t}P^{-1} + |A|\right)(q_i^{n+2} - q_i^{n+1}) = -A^+(q_i^{n+1} - q_{i-1}^{n+1}) - A^-(q_{i+1}^{n+2} - q_i^{n+1}). \tag{35b}$$

7.1 Qualitative optimization

From (35a) and (35b), with (11a) and (11b), in the same way as in Section 3.1, we derive:

$$\mathcal{M}_{\text{downstream}} = \left(\frac{h}{\Delta t}P^{-1} - \mathrm{e}^{-\mathrm{i}\theta}A^{+} + |A|\right)^{-1}\left(\frac{h}{\Delta t}P^{-1} - \mathrm{e}^{\mathrm{i}\theta}A^{-}\right), \tag{36a}$$

$$\mathcal{M}_{\text{upstream}} = \left(\frac{h}{\Delta t}P^{-1} + \mathrm{e}^{\mathrm{i}\theta}A^{-} + |A|\right)^{-1}\left(\frac{h}{\Delta t}P^{-1} + \mathrm{e}^{-\mathrm{i}\theta}A^{+}\right). \tag{36b}$$

We proceed by considering the two highest error frequencies: $|\theta| = \pi$. For both frequencies, with

$$\sigma \equiv \frac{h}{c\Delta t}, \tag{37}$$

(36a) and (36b) can be written out as:

$$\mathcal{M}_{\text{downstream}} = \begin{pmatrix} \sigma\frac{2-M^2}{M^2} + \frac{3}{2} + \frac{1}{2}M & \sigma\frac{1}{M} + \frac{1}{2} + \frac{3}{2}M & 0 \\ \sigma\frac{1}{M} + \frac{1}{2} + \frac{3}{2}M & \sigma + \frac{3}{2} + \frac{1}{2}M & 0 \\ 0 & 0 & \sigma + 2M \end{pmatrix}^{-1} \begin{pmatrix} \sigma\frac{2-M^2}{M^2} - \frac{1}{2} + \frac{1}{2}M & \sigma\frac{1}{M} + \frac{1}{2} - \frac{1}{2}M & 0 \\ \sigma\frac{1}{M} + \frac{1}{2} - \frac{1}{2}M & \sigma - \frac{1}{2} + \frac{1}{2}M & 0 \\ 0 & 0 & \sigma \end{pmatrix}, \tag{38a}$$

$$\mathcal{M}_{\text{upstream}} = \begin{pmatrix} \sigma\frac{2-M^2}{M^2} + \frac{3}{2} - \frac{1}{2}M & \sigma\frac{1}{M} - \frac{1}{2} + \frac{3}{2}M & 0 \\ \sigma\frac{1}{M} - \frac{1}{2} + \frac{3}{2}M & \sigma + \frac{3}{2} - \frac{1}{2}M & 0 \\ 0 & 0 & \sigma + M \end{pmatrix}^{-1} \begin{pmatrix} \sigma\frac{2-M^2}{M^2} - \frac{1}{2} - \frac{1}{2}M & \sigma\frac{1}{M} - \frac{1}{2} - \frac{1}{2}M & 0 \\ \sigma\frac{1}{M} - \frac{1}{2} - \frac{1}{2}M & \sigma - \frac{1}{2} - \frac{1}{2}M & 0 \\ 0 & 0 & \sigma - M \end{pmatrix}. \tag{38b}$$

The corresponding eigenvalues are:

$$(\lambda_1)_{\mathcal{M}_{\text{downstream}}} = \frac{\sigma}{\sigma + 2M}, \quad (\lambda_{2,3})_{\mathcal{M}_{\text{downstream}}} = \frac{\sigma + \sigma^2 - M^2 \pm \sqrt{4\sigma^2(1-M^2) + M^4}}{3\sigma + \sigma^2 + 2M^2}, \tag{39a}$$

$$(\lambda_1)_{\mathcal{M}_{\text{upstream}}} = \frac{\sigma - M}{\sigma + M}, \quad (\lambda_{2,3})_{\mathcal{M}_{\text{upstream}}} = \frac{\sigma + \sigma^2 - M^2 \pm \sqrt{4\sigma^2(1-M^2) + M^4}}{3\sigma + \sigma^2 + 2M^2}. \tag{39b}$$

Note that $(\lambda_{2,3})_{\mathcal{M}_{\text{downstream}}} = (\lambda_{2,3})_{\mathcal{M}_{\text{upstream}}}$. We proceed by considering the eigenvalues for $\lim_{M\downarrow 0}$. With σ a finite (positive) constant this yields

$$\lim_{M\downarrow 0}(\lambda_1, \lambda_2, \lambda_3)_{\mathcal{M}_{\text{downstream}},\, \sigma=\text{constant}} = \left(1, 1, \frac{-\sigma + \sigma^2}{3\sigma + \sigma^2}\right), \tag{40a}$$

$$\lim_{M\downarrow 0}(\lambda_1, \lambda_2, \lambda_3)_{\mathcal{M}_{\text{upstream}},\, \sigma=\text{constant}} = \left(1, 1, \frac{-\sigma + \sigma^2}{3\sigma + \sigma^2}\right). \tag{40b}$$

For $\sigma = \alpha M$ with α a finite (positive) constant it yields

$$\lim_{M\downarrow 0}(\lambda_1, \lambda_2, \lambda_3)_{\mathcal{M}_{\text{downstream}},\, \sigma=\alpha M} = \left(\frac{\alpha}{\alpha + 2}, 1, -\frac{1}{3}\right), \tag{41a}$$

$$\lim_{M\downarrow 0}(\lambda_1, \lambda_2, \lambda_3)_{\mathcal{M}_{\text{upstream}},\, \sigma=\alpha M} = \left(\frac{\alpha - 1}{\alpha + 1}, 1, -\frac{1}{3}\right). \tag{41b}$$

So the choice $\sigma =$ constant yields two maximum eigenvalues equal to one, for both the downstream and upstream sweep. For $\sigma = \alpha M$ with α constant, this number is only one, which probably implies smaller Frobenius matrix norms (see e.g. Chapter 2 from [3]) and hence better smoothing when applying two, three, four, ... Gauss-Seidel sweeps. Note that no function $\sigma = \sigma(M)$ exists which makes the moduli of all three eigenvalues smaller than one for $\lim_{M\downarrow 0}$. We proceed with $\sigma = \alpha M$. In the next section the optimal value of α is derived.

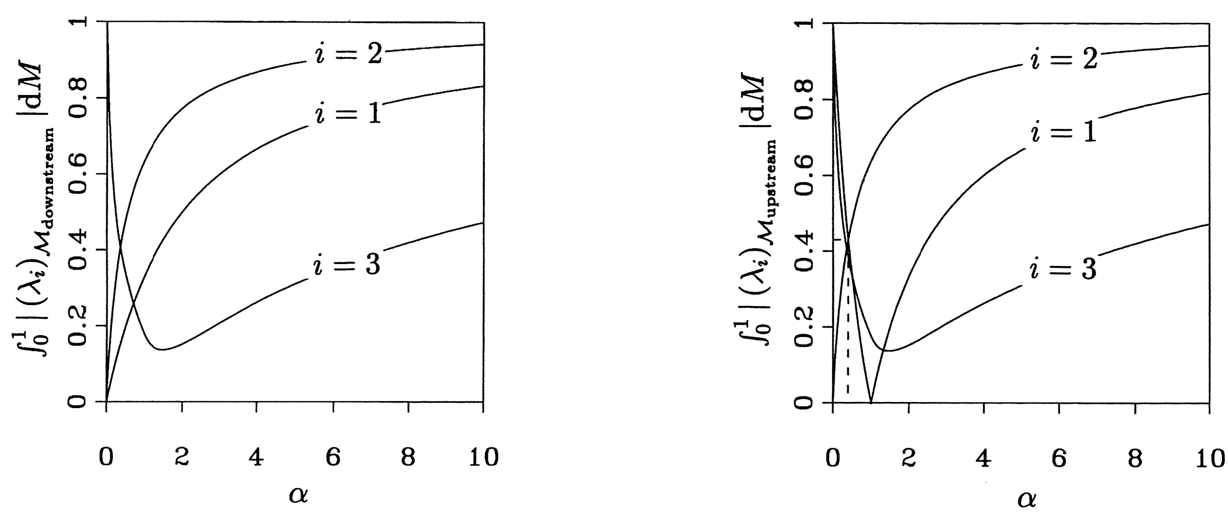

a. Downstream sweep.

b. Upstream sweep.

Figure 2: Integrated moduli of eigenvalues of amplification matrices, for highest error frequencies.

7.2 Quantitative optimization

To optimize α from $\sigma = \alpha M$, we continue to apply Fourier analysis for the highest error frequencies $|\theta| = \pi$, where, as in Section 3.1, we look for spectral radii of the amplification matrices. To avoid Mach-number dependence of α, we consider the moduli of the amplification matrices' eigenvalues integrated over the entire subsonic Mach-number range. (Avoiding Mach-number dependence by taking $\lim_{M \downarrow 0}$ does not allow α-optimization; from (41a) and (41b) it appears that the corresponding spectral radii of both $\mathcal{M}_{\text{downstream}}$ and $\mathcal{M}_{\text{upstream}}$ equal one, for any α.) In Figure 2 the distributions of the aforementioned eigenvalue integrals are depicted over the α-range $[0, 10]$. (Note that since $(\lambda_{2,3})_{\mathcal{M}_{\text{downstream}}} = (\lambda_{2,3})_{\mathcal{M}_{\text{upstream}}}$, the corresponding integrals are the same.) From Figure 2 it can be seen that the optimal value of α follows from $\int_0^1 |(\lambda_1)_{\mathcal{M}_{\text{upstream}}}| dM = \int_0^1 |(\lambda_2)_{\mathcal{M}_{\text{upstream}}}| dM$ (dashed line in Figure 2b), i.e. (after some computer algebra) from:

$$\alpha \frac{-4 + 2\alpha - 2\alpha^2 + \alpha^3 + (5 - 2\alpha^2)\ln\left(\frac{(\alpha+2)^2}{\alpha(2\alpha+1)}\right) - 3\sqrt{1-4\alpha^2}\ln\left(\frac{\sqrt{1-4\alpha^2}+1}{2\alpha}\right)}{(\alpha^2+2)^2} + \frac{\alpha - 1}{\alpha + 1} = 0. \tag{42}$$

From (42), it follows by good approximation that $\alpha = \frac{2}{5}$, and thus as (approximately) optimal σ:

$$\sigma = \frac{2}{5} M. \tag{43}$$

8 Convergence for preconditioned equations

8.1 Error smoothing

Relation (43) implies as (approximately) optimal iteration step Δt:

$$\Delta t = \frac{5}{2} \frac{h}{|u|}, \tag{44}$$

i.e. CFL $= \frac{5}{2}$. We verify the smoothing behavior for this iteration step. This is done over the entire subsonic Mach-number range $(0, 1)$, for the three error frequencies $\theta = \frac{\pi}{2}, \frac{3\pi}{4}$ and π. In Figure 3 the distributions of the corresponding spectral radii are depicted. Recalling from Section 3.1 that the spectral radii of downstream and upstream point Gauss-Seidel relaxation equal one over the entire subsonic Mach-number range, from Figure 3 it appears that the preconditioning does a good job.

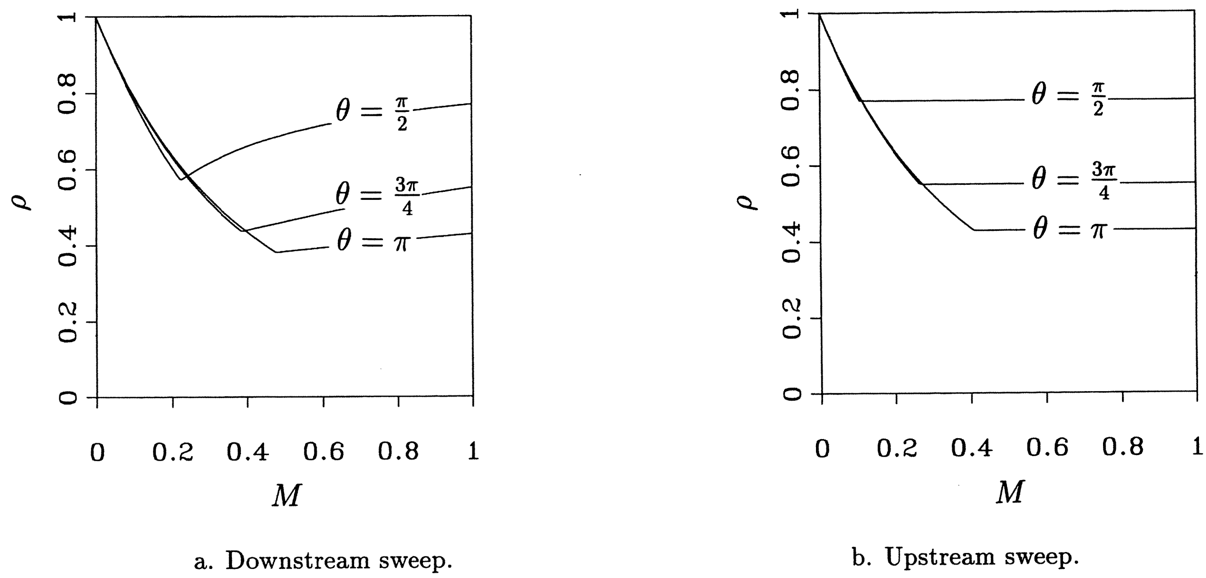

Figure 3: Spectral radii of amplification matrices, for downstream and upstream (approximately optimal) point Gauss-Seidel time-stepping, and three error frequencies.

8.2 Error convection

The locally implicit iteration applied to preconditioned Euler equations may be interpreted as physical time stepping. To do so, for simplicity we consider the common P according to (20) with $w = |u|$. Then, with CFL $= \frac{|u|\Delta t}{h}$, the iteration formulae (35a) and (35b) become

$$(1 + \text{CFL})|A|(q_i^{n+1} - q_i^n) = -A^+(q_i^n - q_{i-1}^{n+1}) - A^-(q_{i+1}^n - q_i^n), \tag{45a}$$

$$(1 + \text{CFL})|A|(q_i^{n+2} - q_i^{n+1}) = -A^+(q_i^{n+1} - q_{i-1}^{n+1}) - A^-(q_{i+1}^{n+2} - q_i^{n+1}). \tag{45b}$$

From (45a) and (45a) it appears that for this common P, the locally implicit time stepping can be directly interpreted as point Gauss-Seidel relaxation with underrelaxation factor $\omega = 1 + \text{CFL}$. I.e., even with CFL $= \mathcal{O}(1)$, (45a) and (45a) can still be interpreted as locally implicit physical time stepping at an infinitely large time step.

9 Conclusions

- Poor convergence of multigrid accelerated point Gauss-Seidel relaxation at low Mach numbers is explained by the relaxation's poor smoothing at low Mach numbers and by the likewise poor entropy-error expulsion across domain boundaries.
- Poor solution accuracy known to occur at low Mach numbers can be explained by means of the modified equation for the 1-D Euler equations, discretized by a first-order accurate flux-difference splitting scheme. For flows with uniformly low Mach numbers, a fix to this inaccuracy is a necessity. For flows of which the global solution error is not affected by the occurrence of low-subsonic flow regions such a fix may not be necessary.
- For the latter flows, implementation of preconditioning in a locally implicit time stepping method with the inverse of the preconditioning matrix working on the time operator, may be practical. It allows the application of an off-the-shelf space discretization method.
- Local-mode analysis shows that optimal high-frequency damping for locally implicit "time" stepping in a Gauss-Seidel way, is obtained for CFL $\approx \frac{5}{2}$. (When preconditioning with the 1-D matrix

$P = \frac{1}{|u|}|A|^{-1}$, the locally implicit "time" stepping boils down to point Gauss-Seidel relaxation with underrelaxation factor $1 + \text{CFL}$.)

- Given the direct availability of the 2-D and 3-D extensions of the 1-D preconditioning matrix analyzed, the present improved solution method is directly extendible to multi-D.

Acknowledgment

Bram van Leer is acknowledged for his suggestions in improving this paper.

References

[1] L. BERS, *Mathematical Aspects of Subsonic and Transonic Gas Dynamics*, Wiley, London, 1958.

[2] M. VAN DYKE, *Perturbation Methods in Fluid Mechanics*, The Parabolic Press, Stanford, 1975.

[3] G.H. GOLUB AND C.F. VAN LOAN, *Matrix Computations*, The John Hopkins University Press, Baltimore, 1989.

[4] P.W. HEMKER AND S.P. SPEKREIJSE, Multiple grid and Osher's scheme for the efficient solution of the steady Euler equations, *Appl. Numer. Math.*, **2**, 475-493, 1986.

[5] B. VAN LEER, W.-T. LEE AND P.L. ROE, Characteristic time-stepping or local preconditioning of the Euler equations, *AIAA-91-1552*, 1991.

[6] A. MAJDA, *Compressible Fluid Flow and Systems of Conservation Laws in Several Space Variables*, Springer, Berlin, 1984.

[7] C.S. MORAWETZ, On the non-existence of continuous transonic flows past airfoils I, *Comm. Pure Appl. Math.*, **9**, 45-68, 1956. II, *ibid.*, **10**, 107-131, 1957. III, *ibid.*, **11**, 129-144, 1958.

[8] S. OSHER AND F. SOLOMON, Upwind difference schemes for hyperbolic systems of conservation laws, *Math. Comput.*, **38**, 339-374, 1982.

[9] P.L. ROE, Approximate Riemann solvers, parameter vectors, and difference schemes, *J. Comput. Phys.*, **43**, 357-372, 1981.

[10] E. TURKEL, Preconditioned methods for solving the incompressible and low speed compressible equations, *J. Comput. Phys.*, **72**, 277-298, 1987.

[11] E. TURKEL, Review of preconditioning methods for fluid dynamics, *Appl. Numer. Math.*, **12**, 257-284, 1993.

[12] E. TURKEL, A. FITERMAN AND B. VAN LEER, Preconditioning and the limit of the compressible to the incompressible flow equations (in preparation).

[13] G. VOLPE, Performance of compressible codes at low Mach numbers, *AIAA J.*, **31**, 49-56, 1993.

[14] P. WESSELING, *An Introduction to Multigrid Methods*, Wiley, Chichester, 1992.

Contents